COMPARISON OF THE MOLDING PARAMETERS EFFECTS ON METAL INJECTION MOLDED SPECIMENS IN THE REAL EXPERIMENTAL AND SIMULATION ENVIRONMENTS

György Ledniczky[1,2,*], Zoltán Weltsch[2]

[1]Department of Innovative Vehicles and Materials, GAMF Faculty of Engineering and Computer Science, John von Neumann University, Kecskemet, Hungary
[2]Department of Road and Rail Vehicles, Szechenyi Istvan University, Gyor, Hungary

*E-mail of corresponding author: ledniczky.gyorgy@nje.hu

György Ledniczky 0009-0001-0949-572X, Zoltán Weltsch 0000-0002-6366-8281

Resume
This article presents a technology that is not widely known. Previous research has investigated the effect of metal injection molding parameters on product shrinkage. The technology is mostly limited by the variations caused by deformation, so it is of paramount importance to focus on shrinkage. Consequently, within this study the injection molding simulations with 17-4PH type material was performed and its results were compared to the previously determined curve characters. The results obtained allow conclusions to be drawn regarding the accuracy of the simulation. Changing the parameters of the injection molding process can significantly affect the shrinkage factor. Changes in mold temperature, melt temperature and holding pressure affect the product dimensions. These parameters are also modified in the simulation setup and compared to the previous real measurements.

Article info
Received 13 November 2023
Accepted 9 January 2024
Online 8 February 2024

Keywords:
metal injection molding
simulation
molding

Available online: https://doi.org/10.26552/com.C.2024.018

ISSN 1335-4205 (print version)
ISSN 2585-7878 (online version)

1 Introduction

Metal Injection Molding (MIM) is a very rapidly developing technology, which can be best compared to a combination of powder metallurgy and plastic injection molding. In recent years, it has spread to a growing number of fields, with applications in a wide variety of areas outside the defense, healthcare and automotive industries. Based on the idea of plastic injection molding, metal powder particles are embedded in a binder and the resulting pellets are pressed into a durable mold by an injection molding machine [1-6]. The resulting granules are commonly called feedstock.

The product that falls out of the mold is the so-called green product. The product in this state is a semi-finished preform, with further steps to achieve metallic properties. So, the next step is to reduce the resulting product in a binder and form an open pore structure, which is true for the entire cross section of the product. In the raw material mixture, it is expected that the individual powder particles, which must be surrounded by a very thin film of binder, are in close contact with each other. There are several types of binder removal, depending on the type of binder system. These can be solvent-based, catalytic, water-based or supercritical binder systems. The bottom line is that the binder must work in such a way that the product is porous, but still has enough binder to hold the particles together.

The binder-reduced product is called the brown product. The product is the most fragile in this state, so it is not recommended to move the product at this stage. In the sintering phase, the product is heated in a high temperature furnace at temperatures below the melting point [7-10]. The process is shown in Figure 1.

Most researchers investigated the influence of the metal powder properties on technology, the rheological properties of the binder and the effect of technology on shrinkage [11-14].

Some researchers analyzed the geometrical effect of the finished workpiece and the limiting value of solvent binder removal [15-17]. These studies contributed greatly to a better understanding of this less known

technology and to a better exploitation of its potential, but beyond that, little attention is paid to preliminary parameterization or modelling.

In the MIM, it is difficult to gain sufficient knowledge for optimal process development from experiments alone. Therefore, we investigate the applicable software to the process in addition to experimental research at Neumann János University, Department of Innovative Vehicles and Materials. A range of necessary equipment, including a computer-controlled injection molding machine, a decomposition furnace and a high-temperature sintering furnace, are organised in an easily adaptable way with data acquisition systems for different physical quantities.

Through their experiments, Barriere et al. have developed a combined application of modelling and numerical simulations to MIM to ensure that parts are free from defects and have the required mechanical properties. Modelling of the injection stage, based on the two-phase flow composition of the powder-binder mixture, has enabled an access to the powder deposition during the injection and an understanding of injection defects [18].

Results from authors' previous research showed that the shrinkage properties of parts manufactured with MIM do not behave like plastics, so the simulations were operformed to investigate its applicability for the characterization of deformations [19-20].

We have started to produce a green product using additive manufacturing linked to the technology presented earlier and are already working on chip testing of sintered test pieces based on previous studies. [21-22].

2 Material

The selected material is martensitic stainless steel, commercially known as 17-4PH, and its main components are listed in Table 1 [23]. This material is commonly used in both MIM and additive manufacturing processes, which is why it is advantageous to use it [24]. Opposed to moststainless steel grades, this exhibits excellent mechanical properties, making it widely utilized in various industrial applications. It is frequently applied in aerospace and space technology, as well as in the oil and gas industry. It is used for the production of screws, springs, nails, gears, and it finds applications in the medical field for manufacturing surgical instruments, as well. The binder used in the process consists of two main components: polypropylene and wax, which are mixed with the metal powder at a ratio of 6 % by weight [25]. The connection between the binder and the metal powder is shown in Figure 2.

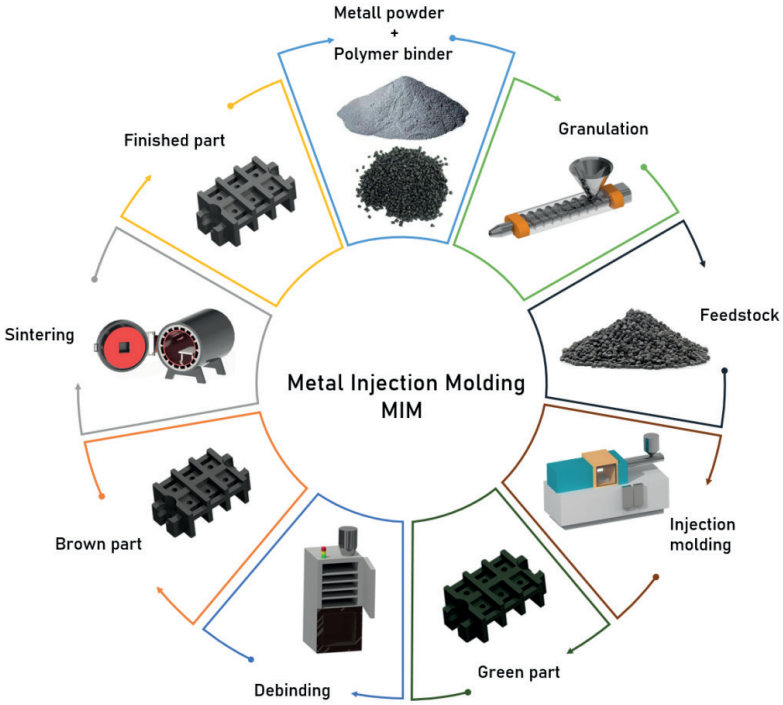

Figure 1 *The metal injection molding process*

Table 1 *17-4PH stainless steel chemical composition [24]*

%	Cr	Mn	Si	Ni	Cu
Min	15.0	--	--	3.50	3.00
Max	17.5	1.00	1.00	5.00	5.00

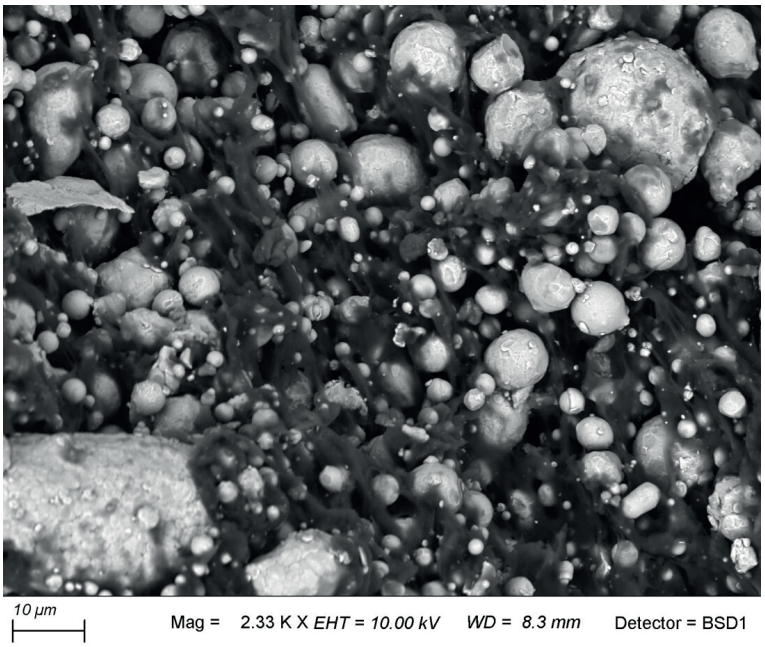

Figure 2 *the SEM image of the 17-4PH powder embedded in binder*

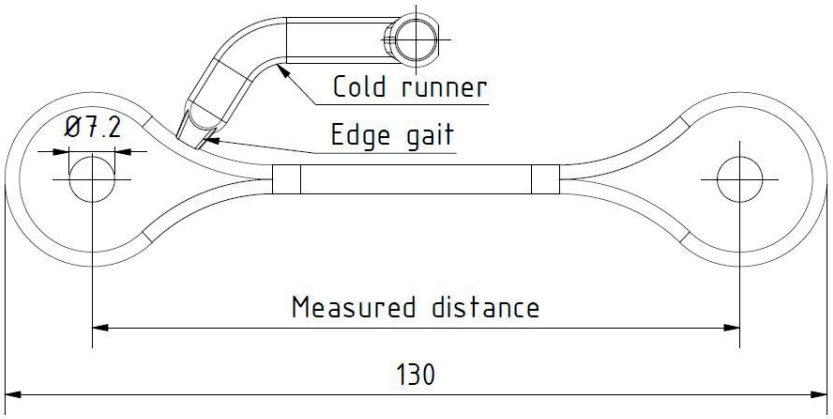

Figure 3 *Test specimen measures*

3 Methodology of injection molding experiments

Molding shrinkage values were determined by measuring the spacing of holes in a test specimen of a dog-bone geometry, Figure 3. It is important to note that the product was tested in "green" condition. In an intermediate step, the row of locking bars in the holes was removed using a reamer. Measurements were taken using an optical measuring device to ensure accuracy.

3.1 Tool used for testing

For conducting the experiments, we employed a specialized molding tool, that was designed for production of a test specimen, weighing around 36 grams. This mold is versatile and can accommodate various types of tests. It is equipped with cooling channels on both sides and includes a central heated nozzle that feeds the mold cavity through a short cold runner.

Figure 4 provides an illustration of the mold utilized in the experiment.

AFT Hungary Ltd generously supplied us with the tool and the opportunity to perform testing with it.

3.2 Molding parameters

The melting temperature was set to correspond to the average processing temperature of the polyethylene (PE) component in the binder, and the holding pressure was set at the midpoint between the two extreme processing limits. The highlighted parameters can be viewed in Table 2. The ideal mold temperature

Figure 4 *The tool used for the test*

Table 2 *The defined processing parameters*

Parameter	Value
Injection volume	6.56 cm^3/s
Injection pressure	903 bar
Postpress time	2 s
Post pressure	827 bar
Cooling time	15 s
Tool temperature	45°
Melt temperature	205 °C

Table 3 *The changed parameters and corresponding values*

Variable	Back press., bar	Tool temp., °C	Melt temp., °C
Deviation -	550	25	195
Deviation -	690	35	200
Average value	827	45	205
Deviation +	965	55	210
Deviation +	1103	65	215
Deviation +	1241	75	220

was determined based on practical observations and experiments. The main objective in designing the experiments was to vary the critical parameters - melt temperature, mold temperature and holding pressure - independently of each other. The variables are shown in Table 3. Consequently, this resulted in production of 16 different process settings. To ensure process stability and thermal equilibrium, the first 5 cases were eliminated. Subsequently, 10 test pieces were produced for each configuration. Out of those, 5 were left as green parts, while the remaining 5 were binder removed and sintered.

Table 4 *The varied parameters and corresponding values*

Parameters type	Set value
Molding Material	Catamold 17-4PH : BASF
Process controller	Process controller defaults
Injection molding machine	Default injection molding machine
Mold material	Tool Steel S-1
Solver parameters	Thermoplastic injection molding solver

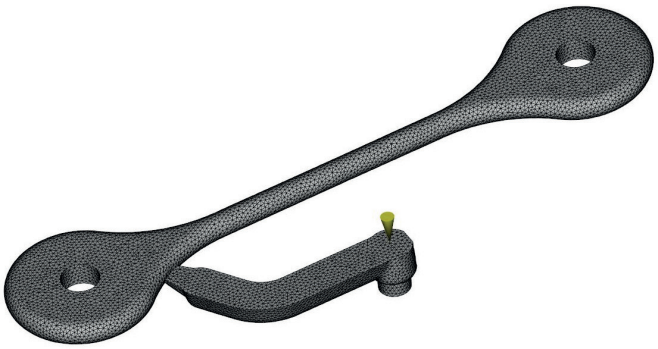

Figure 5 *The simulation model built with a volumetric mesh*

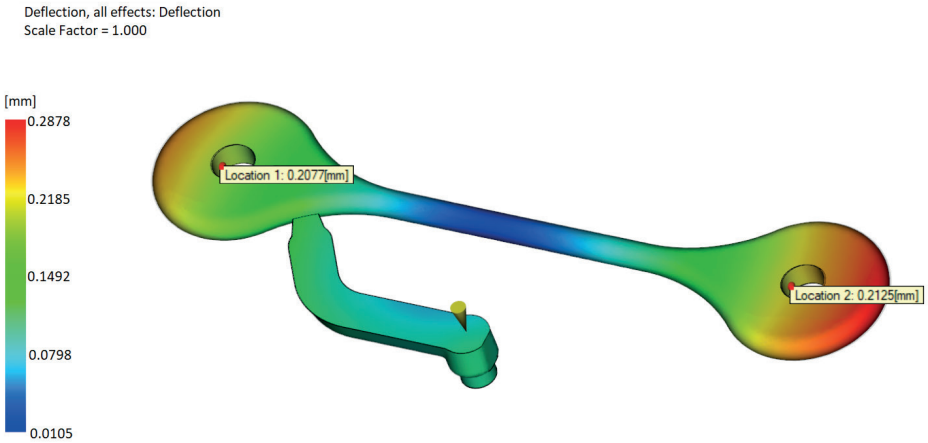

Figure 6 *The simulation model obtained after deformation with the two measurement points*

4 Simulation method

A simulation was performed to evaluate the correlation between the actual measured values and the simulation on the test specimen.

For the simulation, we used Autodesk Moldflow software, a tool specifically designed for simulation of the polymer injection molding, as shown in the set parameters. The simulation included filling and packaging processes. Table 4 shows the set values of the simulation.

The test material consisted of 94 % metal powder (17-4PH) and 6 % binder (PP and wax) granules. In contrast, the raw material selected for the simulation contains 17-4PH metallic powder, but has a catalytic binder removal system (Catamold) manufactured by BASF.

4.1 Definition of shrinkage values in the simulation software

The primary objective of the study was to assess the measurability of linear shrinkage of the product under simulation conditions.

The simulation model was created using a 3D volume mesh consisting of 0.8 mm edge length tetrahedrons, as shown in Figure 5. It consists of 10 layers in thickness.

Figure 5 illustrates the simulation model constructed with the spatial mesh. The product was made with the same gate and inlet as the injection molded part. The basic injection molding parameters, including filling time (injection time), holding pressure and cooling time, remained consistent for both the simulation and real tests.

To determine the linear shrinkage, measurements

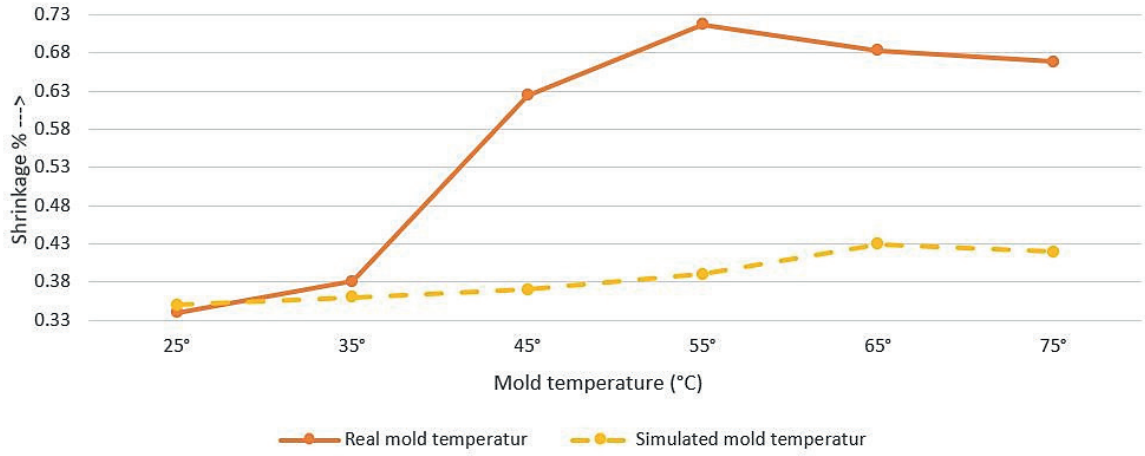

Figure 7 *Real and simulated mold temperature curve*

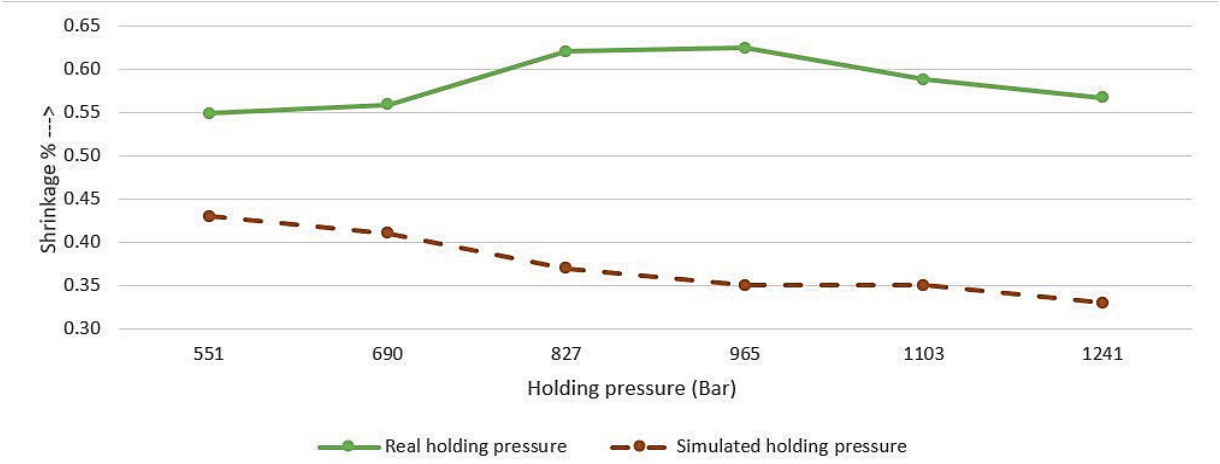

Figure 8 *Real and simulated holding-pressure curve*

were taken on the axial spacing of the holes as shown in Figure 6. The distance (displacement) between the two marked points was evaluated on the simulated image. Based on this distance measurement, the software calculates the shrinkage value based on the product's deformation with shrinkage compensation turned off.

5 Results

The hole distances of samples from the real injection molding tests were measured and the shrinkage value as a function of the parameter was shown in a diagram. The shrinkage value was determined using the following formula.

$$Shrinkage = \left(\frac{tool\ distance}{part\ distance} - 1\right) \cdot 100 \qquad (1)$$

In the simulation, the measurements were carried out according to the same principle and plotted in a diagram.

The main factor affecting the size of the product is the temperature of the mold, as illustrated in Figure 7. Shrinkage ranged from 0.34% to 0.72%, a significant variation, which translates into a dimensional deviation of approximately 0.4 mm over a 100 mm test length.

The solid-line curves always represent the real test results, while the broken-line curves represent the simulation results.

5.1 Modifying the working temperature of the tool

The curve shows an upward trend similar to plastic injection molding, but only up to 55 °C. Beyond this temperature the shrinkage value starts to decrease. During the experiments, it was observed that at higher mold temperatures the products exhibit a "wet" appearance, probably due to the wax extraction from the binder, as shown in Figure 7. Consequently, the metal particles can replace the precipitated wax, resulting in a reduction of the shrinkage factor. It is assumed that this can be quantified based on the percentage composition of the component. For the simulation results it was observed that the shrinkage values show an increase when the temperature is increased, similarly to

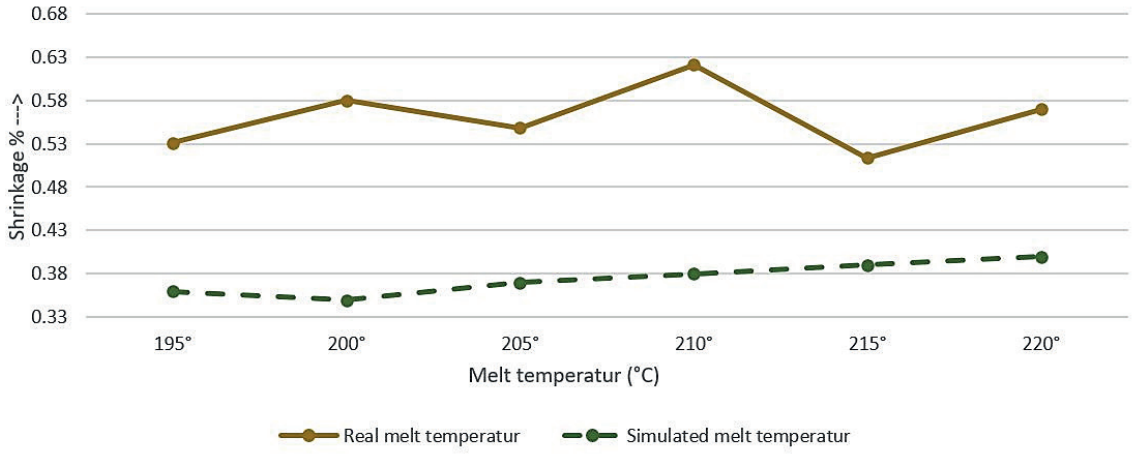

Figure 9 *Real and simulated melt temperature curve*

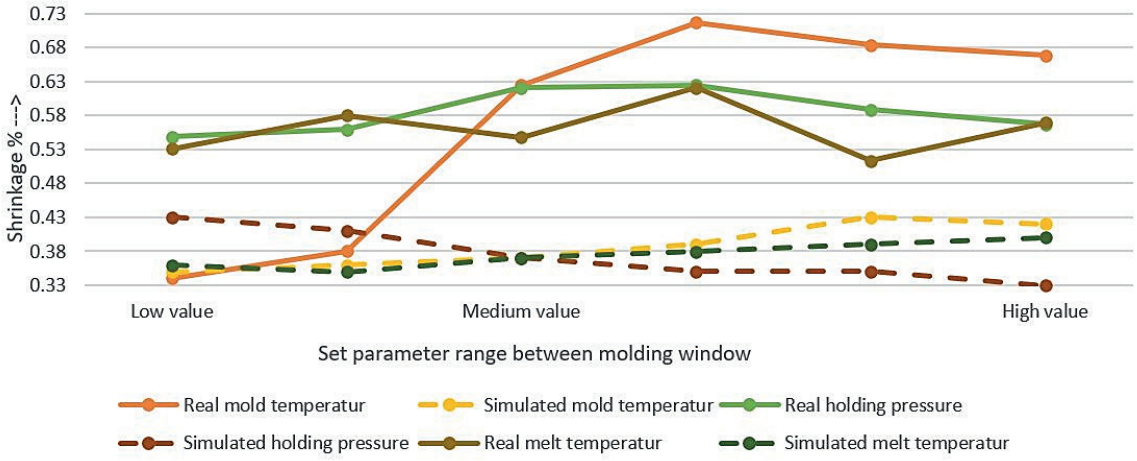

Figure 10 *Combined shrinkage curve*

the real injection molding tests. It is observed that the nature of the curves is similar and peaks at 65 °C mold temperature.

5.2 Modifying the holding-pressure of the injection molding

The relationship between the shrinkage and the change in holding pressure is different as for polymers. The results show that shrinkage reaches a maximum around 900 bar, as shown in Figure 8, leading to reduced shrinkage at higher or lower pressure levels. It is essential to stress that the effect of the applied pressure on shrinkage is much less important than that of the mold temperature. The holding-pressure curve shows a similar character to the injection molding of plastic polymers, but differs significantly from the results obtained in real experiments, both in characteristic and in magnitude.

5.3 Variation of the melt temperature

Deviations from standard plastic processing parameters can be attributed to a variety of factors, but a comprehensive study is needed to fully understand them.

Of all the parameters studied, the variation of the melt temperature had the least effect on product dimensions and the curve showed a significant variation of deviations, as shown Figure 9. The curve generated from the change of the melt temperature shows a similar character to the injection molding of plastic polymers, but differs significantly from the results obtained in real experiments in nature, as well as in magnitude.

5.4 Combined shrinkage factor graph

We combined the results in a common graph to better understand the effect of the different parameter

variations on the shrinkage of the product, Figure 10., Different parameters are plotted on the horizontal axis with a common characteristics, as low, medium and high values. Those values represent the limits of the processing window. A solid line indicates the real results and the broken line indicates the simulation results.

6 Summary and conclusions

The experiments were carried out with the aim of facilitating the simultaneous application of modelling and numerical simulations and the comparison of the actual measured results within the MIM process. To minimize the deformation of the MIM parts, it is important to know the effects of injection molding parameters.

Summary of research results:

- Simulation results at lower temperatures are closer to real measurements, however,
- with increasing temperature, there was a significant discrepancy between the simulation and real tests.
- The variation of the holding-pressure parameter shows a different characteristics.
- The difference in the magnitude of the discrepancies may be caused by the binder system not being exactly the same, but the out-of-character behavior may be caused by the simulation model itself. The assumption is supported by the correspondence of the characteristics of the curves obtained from the simulation to the properties characteristic of the polymers, which, in the present case for metal injection molding, can only be accepted conditionally if a material with a solvent binder system is processed with the used injection molding machine.
- To clarify these discrepancies, the exact material properties required for the simulations should be measured in later stages.

Acknowledgements

We thank AFT-Hungary Kft. for their generous help in securing the raw materials and technology.

Project no. TKP2021-NVA-23 has been implemented with the support provided by the Ministry of Technology and Industry of Hungary from the National Research, Development and Innovation Fund, financed under the TKP2021-NVA funding scheme.

This work was supported by the Janos Bolyai Research Scholarship of the Hungarian Academy of Sciences (ZW).

Conflicts of interest

The authors declare that they have no known competing financial interests or personal relationships that could have appeared to influence the work reported in this paper.

References

[1] GERMAN, R. M., HENS, K. F. Key issues in powder injection molding. *American Ceramic Society Bulletin*. 1991, **70**(8), p. 1294-1302. ISSN 0002-7812.

[2] GERMAN, R. M. Technological barriers and opportunities in powder injection molding. *Powder Metallurgy International*. 1993, **25**(4), p. 165-169. ISSN 0048-5012.

[3] KULKARNI, K. M. Future looking bright for PIM. *Metal Powder Report* [online]. 2000, **55**(10), p. 40-42. ISSN 0026-0657. Available from: https://doi.org/10.1016/S0026-0657(00)80068-5

[4] BALLARD, C., ZEDALIS, M. Advances in powder injection molding. In: Annual Technical Conference ANTEC: proceedings. Vol. 1. 1998. p. 358-361.

[5] HAUCK, P. A. Powder injection molding: current and long term outlook. *International Journal of Powder Metallurgy*. 2000, **36**(3), p. 29-30. ISSN 0888-7462.

[6] GERMAN, R. M. Scientific status of metal powder injection molding. *International Journal of Powder Metallurgy*. 2000, **36**(3), p. 31-36. ISSN 0888-7462.

[7] HONG, S., KANG, J., YOON, K. Correlation between thermal contact resistance and filling behavior of a polymer melt into multiscale cavities in injection molding. *International Journal of Heat and Mass Transfer* [online]. 2015, **87**, p. 222-236. ISSN 0017-9310, eISSN 1879-2189. Available from: https://doi.org/10.1016/j.ijheatmasstransfer.2015.03.061

[8] LUCCHETTA, G., MASATO, D., SORGATO, M., CREMA, L., SAVIO, E. Effects of different mold coatings on polymer filling flow in thin-wall injection molding. *CIRP Annals* [online]. 2016, **65**(1), p. 537-540. ISSN 0007-8506, eISSN 1726-0604. Available from: https://doi.org/10.1016/j.cirp.2016.04.006

[9] SARDARIAN, M., MIRZAEE, O., HABIBOLAHZADEH, A. Influence of injection temperature and pressure on the properties of alumina parts fabricated by low pressure injection molding (LPIM). *Ceramics International* [online]. 2017, **43**(6), p. 4785-4793. ISSN 0272-8842, eISSN 1873-3956. Available from: https://doi.org/10.1016/j.ceramint.2016.11.208

[10] ZHANG, Y., PEDERSEN, D. B., GOTJE, A. S., MISCHKOT, M., TOSELLO, G. A Soft Tooling process chain employing Additive Manufacturing for injection molding of a 3D component with micro pillars. *Journal of Manufacturing Processes* [online]. 2017, **27**, p. 138-144. ISSN 1526-6125, eISSN 2212-4616. Available from: https://doi.org/10.1016/j.jmapro.2017.04.027

[11] DE SOUZA, J. P., ATRE, S. V., SURI, P. K., THOMAS, J. A., GERMAN, R. M. Understanding homogeneity of powder-polymer mixtures-effect of mixing on tungsten powder injection molding feedstock. *Metalurgia e Materials*. 2003, **59**(Suppl. 7), p. 16-19. ISSN 0104-0898.

[12] SUPATI, R., LOH, N. H., KHOR, K. A., TOR, S. B. Mixing and characterization of feedstock for powder injection molding. *Materials Letters* [online]. 2000, **46**(2-3), p. 109-114. ISSN 0167-577X, eISSN 1873-4979. Available from: https://doi.org/10.1016/S0167-577X(00)00151-8

[13] DROPMANN, M. C., STOVER, D., BUCHKREMER, H. P., DIEHL, W., VASSEN, R. Injection molding with ultra high solids loading. In: Powder Injection Molding Symposium: proceedings. Vol. 92. 1992. p. 287-293.

[14] LI, Y., JIANG, F., ZHAO, L., HUANG, B. Critical thickness in binder removal process for injection molded compacts. *Materials Science and Engineering: A* [online]. 2003, **362**(1-2), p. 292-299. ISSN 0921-5093, eISSN 1873-4936. Available from: https://doi.org/10.1016/S0921-5093(03)00613-0

[15] WESTCOT, E. J., BINET ANDRANDALL, C., GERMAN, R. M., In situ dimensional change, mass loss and mechanisms for solvent debinding of powder injection molded components. *Powder Metallurgy* [online]. 2003, **46**(1), p. 61-67. ISSN 0032-5899, eISSN 1743-2901. Available from: https://doi.org/10.1179/003258903225010442

[16] LIU, D.-M., TSENG, W. J. Influence of solids loading on the green microstructure and sintering behaviour of ceramic injection moldings. *Journal of Materials Science* [online]. 1997, **32**(24), p. 6475-6481. ISSN 0022-2461, eISSN 1573-4803. Available from: https://doi.org/10.1023/A:1018646824219

[17] TSENG, W. J. Statistical analysis of process parameters influencing dimensional control in ceramic injection molding. *Journal of Materials Processing Technology* [online]. 1998, **79**(1-3), p. 242-250. ISSN 0924-0136, eISSN 1873-4774. Available from: https://doi.org/10.1016/S0924-0136(98)00019-3

[18] BARRIERE, T., LIU, B., GELIN, J. C. Determination of the optimal process parameters in metal injection molding from experiments and numerical modeling. *Journal of Materials Processing Technology* [online]. 2003, **143-144**, p. 636-644. ISSN 0924-0136, eISSN 1873-4774. Available from: https://doi.org/10.1016/S0924-0136(03)00473-4

[19] LEDNICZKY, G., WELTSCH, Z. Molding simulation of metal injection molded automotive parts. In: 38th International Colloquium on Advanced Manufacturing and Repair Technologies in Vehicle Industry: proceedings. 2023. ISBN 9789639058484, p. 51-54.

[20] LEDNICZKY, G., WELTSCH, Z. Effects of injection Molding Parameters on the Produced Parts / A femfroccsontes parametereinek hatasa a gyartott alkatreszekre (in Hungarian). *Acta Materialia Transylvanica* [online]. 2023, **6**(1), p. 33-37. ISSN 2601-1883. Available from: https://doi.org/10.33923/amt-2023-01-06

[21] KONYA, G., FICZERE, P. The effect of layer thickness and orientation of the workpiece on the micro- and macrogeometric properties and the machining time of the part during 3D printing. *Periodica Polytechnica Mechanical Engineering* [online]. 2023, **67**(2), p. 143-150. eISSN 1587-379X. Available from: https://doi.org/10.3311/PPme.21473

[22] BOGNAR, A., KUN, K. Design of a heating unit for photopolymerization-based 3D printing technology. In: 38th International Colloquium on Advanced Manufacturing and Repair Technologies in Vehicle Industry: proceedings. 2023. p. 46-50.

[23] Ametek specialty metal products. Specialty powders. 17.4 PH alloy powder - Ametek special metal products [online] [accessed 2013-06-21]. Available from: https://www.powderclad.com/products/specialty-powders/17-4-ph-alloy-powder

[24] SINGH, G., MISSIAEN, J.-M., BOUVARD, D., CHAIX, J.-M. Additive manufacturing of 17-4 PH steel using metal injection molding feedstock: analysis of 3D extrusion print-ing, debinding and sintering. *Additive Manufacturing* [online]. 2021, **47,** 102287. ISSN 2214-8604, eISSN 2214-7810. Available from: https://doi.org/10.1016/j.addma.2021.102287

[25] HAMIDI, M. F. F. A., HARUN, W. S. W., KHALIL, N. Z., GHANI, S. A. C., AZIR, M. Z. Study of solvent debinding parameters for metal injection molded 316L stainless steel. *IOP Conference Series: Materials Science and Engineering* [online]. 2017, **257**, 012035. ISSN 1757-899X. Available from: https://doi.org/10.1088/1757-899X/257/1/012035